This is the accepted manuscript (postprint) of the following article:
Aghamohammadi, H., Abbandanak, S. N. H., Eslami-Farsani, R., & Siadati, S. H. (2018). Effects of various aluminum surface treatments on the basalt fiber metal laminates interlaminar adhesion. *International Journal of Adhesion and Adhesives*, *84*, 184-193.
https://doi.org/10.1016/j.ijadhadh.2018.03.005

Effects of various aluminum surface treatments on the basalt fiber metal laminates interlaminar adhesion

Hamed Aghamohammadi, **S. Navid Hosseini Abbandanak, Reza Eslami-Farsani*, S. M. Hossein Siadati**

Faculty of Materials Science and Engineering, K. N. Toosi University of Technology, Tehran, Iran.

Abstract

Fiber metal laminates (FMLs) are a new class of advanced materials consisting of metal and fiber reinforced polymer layers. Surface treatment of the metal layers can have significant effects on the interlaminar properties and thus the overall properties of FMLs. The aim of this study was to apply four different surface treatment methods on the aluminum layers and investigate their effects on the flexural behavior of a FML made up of Al2024, basalt fibers and epoxy Epon 828. To study the surface morphologies and fracture surface of samples, scanning electron microscopy (SEM), optical microscopy (OM) and profilometry were utilized. Results of the four methods applied, showed that the mechanical abrasion and alkaline etching treatments were not found suitable for enhancing the flexural properties due to weak interfacial adhesive bonding. OM images revealed that the adhesive failure was the failure type of mechanical abrasion and alkaline treated samples. On the other hand, Forest Products Laboratory etching (FPL-etching) and anodizing treatments caused significant improvements in the flexural properties. The improvements are attributed to the formation of surface oxide layers containing microscale pits. The microscale pits provided appropriate sites for the penetration of the polymer resin, which caused strong interfacial bonding

* Corresponding author. E-mail address: eslami@kntu.ac.ir

This is the accepted manuscript (postprint) of the following article:
Aghamohammadi, H., Abbandanak, S. N. H., Eslami-Farsani, R., & Siadati, S. H. (2018). Effects of various aluminum surface treatments on the basalt fiber metal laminates interlaminar adhesion. *International Journal of Adhesion and Adhesives*, *84*, 184-193.
https://doi.org/10.1016/j.ijadhadh.2018.03.005

by mechanical interlocking mechanism. Moreover, SEM and OM images indicated that the main failure type of FPL-etching and anodized samples was the cohesive failure.

Keywords: FMLs, Surface treatment, Anodizing, Flexural properties

1- Introduction

Outstanding properties of fiber reinforced polymers (FRPs) have rendered them as effective materials for automotive applications but their weak interlaminar shear strength has made them susceptible to impact loading. Improvement in impact response of FRPs can be achieved using fiber metal laminates (FMLs) which are a new group of hybrid materials. FMLs consist of alternately stacked layers of thin metal sheets that are held together by the conventional FRPs. The main advantages of FMLs include high wear strength, impact resistance and the fatigue and corrosion properties that are provided by the presence of FRPs. Glass, carbon and aramid fibers are known as the most common fibers used in FMLs [1, 2].

Basalt fibers are a type of natural fibers obtained from basaltic volcanic rock. Basalt fibers have several outstanding properties such as high chemical stability, good resistance to high temperature, high mechanical strength, non-toxicity, non-combustibility, etc. Basalt fibers are produced using a similar production technology as for glass fibers. While glass fibers are produced from a complex batch of materials, basalt fibers are made from only melting of basalt rock and consequently are cheaper. Considering these reasons, several studies have reported on using basalt fibers instead of glass fibers as the reinforcement phase in polymer matrix composites [3-5].

Regarding the FMLs, however, few researchers have studied their mechanical behavior with basalt fibers as the reinforcement. The first study on the mechanical behavior of basalt FMLs was carried out in 2011 by Khalili et al. [5]. They investigated the tensile and bending properties of basalt fibers reinforced epoxy (BFRE) and basalt FMLs. They reported that the energy absorption of basalt FMLs was much higher than that of BFRE. In another study, the low velocity impact behavior of basalt FMLs was investigated by Farsani et al. [3]. Their results demonstrated that the energy absorption of basalt FMLs were higher compared to BFRP.

For best performance, there should be strong adhesion between the metal sheets sandwiching the FRPs. This strong adhesion creates fiber bridging which leads to load transfer from the fracturing metal layer to the stronger fibers in the adjacent FRP layers. This phenomenon provides superior properties by hindering crack initiation and crack growth in the FMLs, conveying significant effect on the strength, stiffness, toughness and failure mode of the FMLs [6-8].

Various methods have been proposed in order to create strong interfacial adhesion, which could improve the mechanical properties of the FMLs. Surface morphology of the metal layers plays a significant role on the adhesion between the metal sheets and FRPs. Surface pretreatment of metals through increasing the number of active chemical groups leads to optimizing the interfacial adhesion. In the literature, various methods have been proposed: mechanical (mechanical abrasion and grit-blasting), chemical etching, anodizing, coupling agent, etc. [9].

Mechanical methods cause more interaction between metal and polymer through increasing the surface area for bonding. For example, Mohamad et al. [10] used different grit size sandpaper to investigate the effect of surface roughness on the mechanical behavior of carbon fiber aluminum laminates (CARALL). They concluded that higher surface roughness of the aluminum surfaces created better adhesion/mechanical interlocking between aluminum and carbon fiber reinforced polymers (CFRPs), resulting in higher strength within the FML system.

The application of chemical etching and anodizing methods cause modification of the chemical nature of metal's surface. The most common chemical and/or electrochemical methods that have been used for enhancing adhesive interfacial bonding are Forest Product Laboratory etching (FPL-etching), sulfo-ferric etching (P2-etching), chromic acid anodizing (CAA) and phosphoric acid anodizing (PAA). A porous nanostructure is formed at the surface of metal upon using these methods. Infiltration of the polymer into the porous structure provides a good adhesion between metal and polymer. A growing body of literature has studied the surface morphology of aluminum after various chemical and electrochemical methods [9, 11, 12].

Some preliminary work was carried out in the early 1980s [11, 12]. For example, Venables et al. [12] studied the oxide morphology of the FPL-etching, CAA and PAA surfaces. They showed that the surface morphologies of these methods are nearly same but differ in terms of pore diameter and wall thickness. They showed that the surface roughness and density of oxide layer that formed after CAA are higher than those for PAA and FPL. In another study, Arrowsmith and Clifford [11] studied the effect of sulfuric acid anodizing (SAA) and PAA on the surface morphology of aluminum using high resolution SEM. They showed that the SAA led to the formation of an anodic oxide layer with the cell diameter of 55 nm and pore diameter of 23.5 nm. In addition, they indicated that the PAA produced much wider pores than those for SAA.

In a number of studies, the effects of different surface treatments on the mechanical behavior of FMLs have been investigated. Lawcock et al. [13] conducted a comparative study on the effects of two surface treatments of P2-etching and modified FPL-etching on the mechanical behavior of CARALL. They reported that the FPL-etching promoted better adhesion between the aluminum and FRP layers, exhibiting interfacial toughness six times higher as compared to the P2-etching. In another study, Prolongo et al. [14] studied the effect of various surface treatments of abrasion, alkaline, FPL and P2 on the morphologies of Al 1050 and Al 2024 and their effects upon the adhesion strength of single lap joints. Their results showed that the Al 2024 is more susceptible to corrosion than Al 1050. They demonstrated that the application of P2 and FPL methods have significant effect on improving the adhesion strength of single lap joints, compared to the abrasion and alkaline methods.

The effects of three different anodizing electrolytes of H_3PO_4, H_2SO_4 and HNO_3 on the mechanical properties of CARALL were examined by Mohamad et al. [15]. Higher strength of samples prepared by H_3PO_4 surface treatment compared with H_2SO_4 and HNO_3 surface treatments have been reported and this behavior has mainly been attributed to deeper infiltration of resin in the porous channels created by the H_3PO_4 anodizing treatment. Xu et al. [8] studied the effects of different parameters of PAA such as electrolyte concentration, time, temperature, etc. on the adhesion behavior of epoxy and aluminum alloy. They concluded that, because of two different mechanisms of resin infiltration, increasing of roughness and apparent surface energy are not always suitable approaches to achieving adhesive bonding. Therefore, there should be an optimum correlation between roughness and apparent surface energy for adhesive bonding.

The aim of this study was to investigate the effects of different surface treatment methods on the flexural properties of FMLs based on 2024 aluminum alloy and furnace basalt fibers reinforced epoxy resin. To the best of the authors' knowledge, the effects of various surface treatments on the flexural behavior of basalt FMLs have not been reported in the literature.

This is the accepted manuscript (postprint) of the following article:
Aghamohammadi, H., Abbandanak, S. N. H., Eslami-Farsani, R., & Siadati, S. H. (2018). Effects of various aluminum surface treatments on the basalt fiber metal laminates interlaminar adhesion. *International Journal of Adhesion and Adhesives*, *84*, 184-193.
https://doi.org/10.1016/j.ijadhadh.2018.03.005

2- Experimental

2-1- Materials

The materials used for fabrication of samples were aluminum alloy grade 2024-T3 with 0.5 mm thickness, basalt fibers (BAS 350.1270.A, Basaltex, Belgium) and epoxy resin (Epon 828, with hardener TETA). The resin to hardener ratio was 100:13 by weight, as recommended by the manufacturer.

2-2- Surface treatment of aluminum alloy

Prior to lamination, four surface treatment methods were applied on the aluminum alloy sheets: mechanical abrasion, alkaline etching, FPL-etching and SAA. The mechanical abrasion method involved hand abrasion by sandpaper with grit size of 80 followed by cleaning with acetone to remove dust, grease, oil, rust, etc. The alkaline etching treatment involved cleaning by acetone followed by sample immersion in NaOH solution (0.2%) for 2 min.

In the FPL-etching method, the chemical composition of the etching solution consisted of 33.7 g/l sodium dichromate ($Na_2Cr_2O_7$) and 374.5 g/l sulfuric acid, according to the ASTM D2674. The aluminum samples were first cleaned by acetone, then immersed in NaOH solution (0.2%) for 2 min and etched for 30 min at 60 ºC. After etching, the samples were immersed in distilled water for 5 min. Finally, the samples were placed in a furnace for one hour at 50 ºC.

In the SAA method, the samples were first cleaned by acetone, then immersed in NaOH solution (0.2%) for 2 min and then immersed in distilled water for 10 min. To the distilled water, 1 ml HNO_3 (63%) was added and the samples were deoxidized and washed. Then, the SAA process was done (0.5 molar, 0.15 A, 20 ℃) at different times (10, 20 and 30 min) and then samples were washed. Finally, the aluminum samples were placed in the furnace for one hour at 50 ℃.

2-3- Fabrication of FMLs

The FMLs with 2/1 configuration and dimensions of 15×2.5×0.19 cm^3 (length × width × thickness) were fabricated by hand lay-up method. The interlayer consisted of 4 layers of basalt fibers reinforced epoxy resin. After laminating, the samples were placed into a mold for the curing

This is the accepted manuscript (postprint) of the following article:
Aghamohammadi, H., Abbandanak, S. N. H., Eslami-Farsani, R., & Siadati, S. H. (2018). Effects of various aluminum surface treatments on the basalt fiber metal laminates interlaminar adhesion. *International Journal of Adhesion and Adhesives*, *84*, 184-193.
https://doi.org/10.1016/j.ijadhadh.2018.03.005

step at 0.15 MPa and ambient temperature. Applying pressure resulted in reduction of bubbles and removal of excess resin. The specimen codes are given in Table 1.

Table 1. Specimen's code

Specimen	Code
Mechanical abrasion	MA
Alkaline treated	Alkaline
10 min sulfuric acid anodizing	SAA10
20 min sulfuric acid anodizing	SAA20
30 min sulfuric acid anodizing	SAA30
FPL-etching	FPL

2-4- Microstructural analysis

Surface morphologies of the pretreated aluminum sheets were studied by scanning electron microscopy (TESCAN SEM); to perform this analysis, the samples were cut into 1.5×1.5 cm^2 size specimens. Moreover, the fracture analyses of samples were carried out using optical microscopy (Meiji Techno OM) and SEM (Quant FEG 250) images.

2-5- Flexural testing

Three-point flexural bend test was conducted at ambient temperature according to ASTM D790. KOPA Universal Testing Machine TB-10T was employed to conduct the test. The flexural strength and flexural strain of samples were calculated by equations (1) and (2), respectively.

$$\sigma_f = \frac{3PL}{2bd^2} \quad (1)$$

$$\varepsilon_f = \frac{6Dd}{L^2} \quad (2)$$

This is the accepted manuscript (postprint) of the following article:
Aghamohammadi, H., Abbandanak, S. N. H., Eslami-Farsani, R., & Siadati, S. H. (2018). Effects of various aluminum surface treatments on the basalt fiber metal laminates interlaminar adhesion. *International Journal of Adhesion and Adhesives*, *84*, 184-193.
https://doi.org/10.1016/j.ijadhadh.2018.03.005

Where σ_f is the flexural strength (MPa), ε_f is the flexural strain, P is the maximum load (N), L is the support span (mm), b is the width of beam tested (mm), d is the depth of beam tested (mm) and D is the maximum deflection of the center of the beam (mm). In addition, the toughness was calculated by measuring the surface area under the stress-strain curve.

2-6- Roughness testing

To characterize the effect of anodizing time (5 min to 60 min) on the surface roughness of samples, the Surtronic + 3 profilometer according to the DIN EN IS 0274:1998 was used. Prior to roughness testing, samples were kept in sonication bath and acetone for 20 min. For each specimen, five measurements at different locations were performed using a cut-off length of 0.8 mm and an evaluation length of 4 mm and average values reported.

3- Results and Discussion

3-1- SEM results

Surface morphology of the Al2024 alloy sheet surface treated with mechanical abrasion is illustrated in Fig. 1. It is evident that the mechanical abrasion treatment led only to the formation of macro-size roughness on the Al2024 surface. Fig. 2 shows the effect of alkaline treatment on the Al2024 and it is obvious that a rough and flake-like surface took shape. The surface morphologies of the samples treated with SAA at 10, 20 and 30 min are presented in Figs. 3, 4 and 5, respectively. Upon anodizing, it is reported that a porous structure of an alumina layer formed on the Al2024 surface [13]. However, it is clear that the oxide layer of aluminum after SAA consists of microscale pits caused by etching treatment.

This is the accepted manuscript (postprint) of the following article:
Aghamohammadi, H., Abbandanak, S. N. H., Eslami-Farsani, R., & Siadati, S. H. (2018). Effects of various aluminum surface treatments on the basalt fiber metal laminates interlaminar adhesion. *International Journal of Adhesion and Adhesives*, *84*, 184-193.
https://doi.org/10.1016/j.ijadhadh.2018.03.005

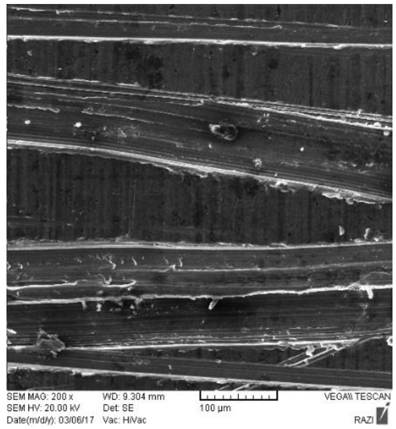

Fig. 1. The surface morphology of Al2024 after mechanical abrasion.

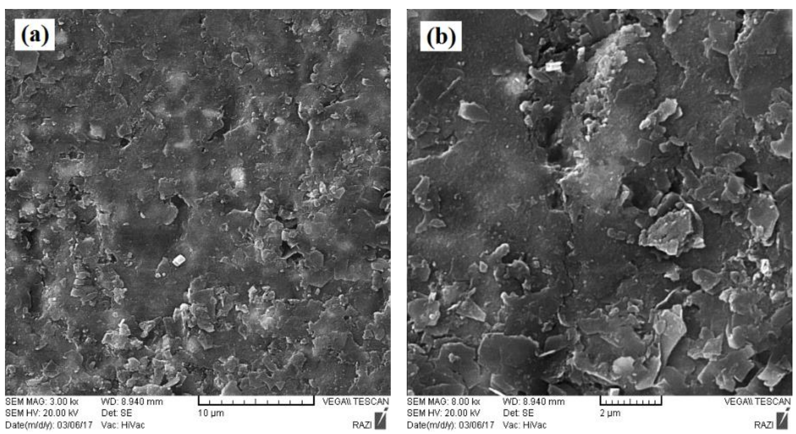

Fig. 2. The surface morphology of Al2024 after alkaline treatment at different magnifications.

This is the accepted manuscript (postprint) of the following article:
Aghamohammadi, H., Abbandanak, S. N. H., Eslami-Farsani, R., & Siadati, S. H. (2018). Effects of various aluminum surface treatments on the basalt fiber metal laminates interlaminar adhesion. *International Journal of Adhesion and Adhesives*, *84*, 184-193.
https://doi.org/10.1016/j.ijadhadh.2018.03.005

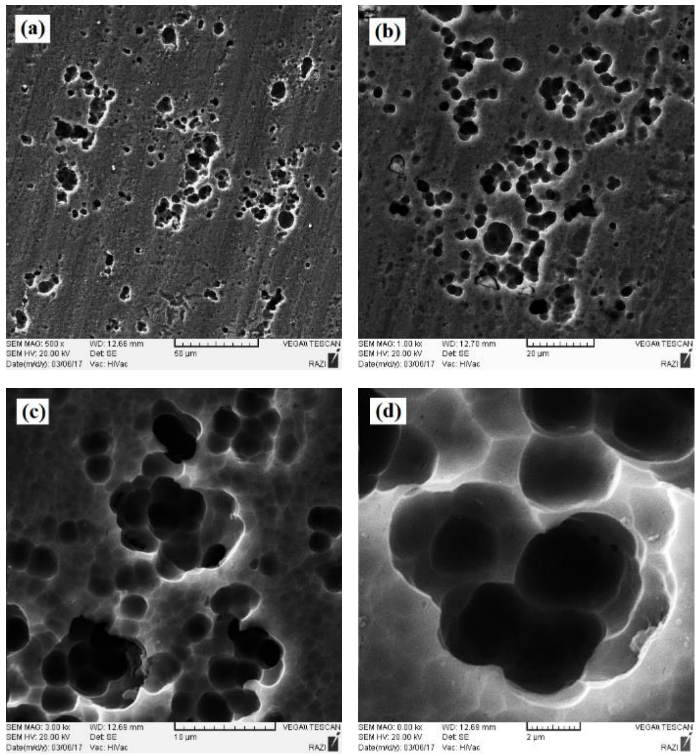

Fig. 3. The surface morphology of Al2024 after 10 min anodizing at different magnifications.

This is the accepted manuscript (postprint) of the following article:
Aghamohammadi, H., Abbandanak, S. N. H., Eslami-Farsani, R., & Siadati, S. H. (2018). Effects of various aluminum surface treatments on the basalt fiber metal laminates interlaminar adhesion. *International Journal of Adhesion and Adhesives*, *84*, 184-193.
https://doi.org/10.1016/j.ijadhadh.2018.03.005

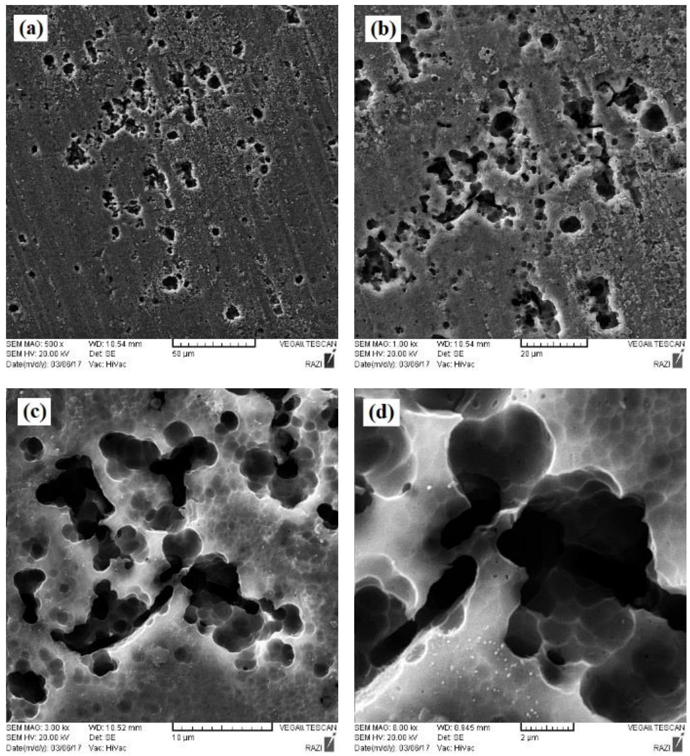

Fig. 4. The surface morphology of Al2024 after 20 min anodizing at different magnifications.

This is the accepted manuscript (postprint) of the following article:
Aghamohammadi, H., Abbandanak, S. N. H., Eslami-Farsani, R., & Siadati, S. H. (2018). Effects of various aluminum surface treatments on the basalt fiber metal laminates interlaminar adhesion. *International Journal of Adhesion and Adhesives*, *84*, 184-193.
https://doi.org/10.1016/j.ijadhadh.2018.03.005

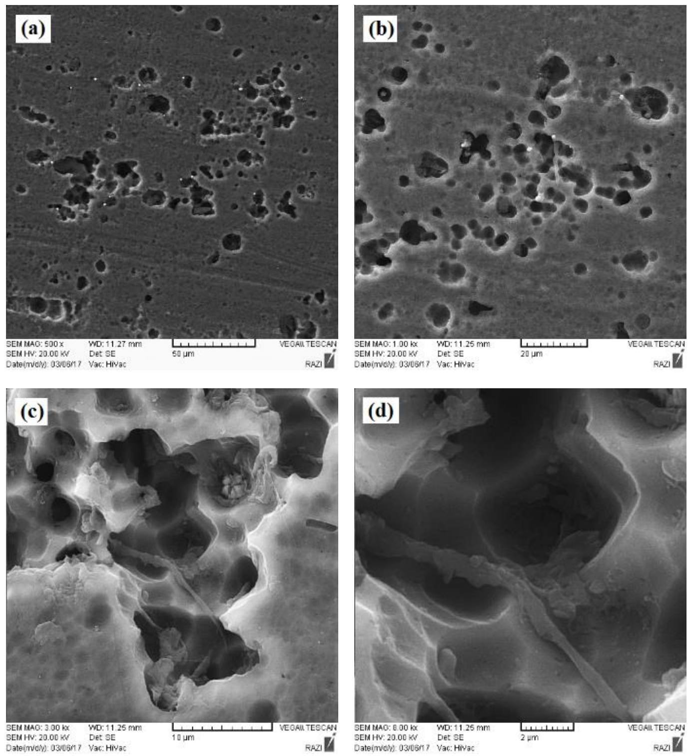

Fig. 5. The surface morphology of Al2024 after 30 min anodizing at different magnifications.

As mentioned in the literature, the anodizing treatments of aluminum leads to the formation of an oxide layer with nanoscale pores. The appearance of microscale pits can be attributed to the presence of copper in Al 2024. It is well-known that the copper in this alloy is in two forms of solid solution and $CuAl_2$. Moreover, it is important to note that the electrochemical activity of aluminum is higher than $CuAl_2$. Therefore, the appearance of microscale pits on the aluminum surface is related to the galvanic corrosion between aluminum and $CuAl_2$. These findings are in good agreement with previous findings [8, 16, 17]. For example, to characterize the role of copper on the oxide morphology of aluminum, surface morphology of Al 2024 and Al 1100 after various surface treatments was carried out by Fin et al. [17]. Their results showed that the cell diameter of Al 2024 is higher than that for Al 1100, after all the treatments.

In another study, Datta et al. [16] investigated the influence of copper contents on the morphology of etched and anodized Al-Cu alloys. Their results demonstrated that with copper content increasing, the pit size of samples increased after anodizing. For example, in sample

This is the accepted manuscript (postprint) of the following article:
Aghamohammadi, H., Abbandanak, S. N. H., Eslami-Farsani, R., & Siadati, S. H. (2018). Effects of various aluminum surface treatments on the basalt fiber metal laminates interlaminar adhesion. *International Journal of Adhesion and Adhesives*, *84*, 184-193.
https://doi.org/10.1016/j.ijadhadh.2018.03.005

containing 5.5 wt.% copper, the pit's diameter of 25 µm was observed. Saenz de Miera et al. [18] studied the role of real and model second phase particles on the morphology of the aluminum alloys after anodizing. In consistent to the Datta et al. findings, their results demonstrated that with increasing the copper content of alloys, the rate of second phase dissolution increases. They said that the oxygen evaluation and associated cyclic disruption of the oxide layer increased when the copper content increased.

However, evident in the SEM images is the impact of time; the average pit diameter increased in size, as the anodizing time increased, and also the pit became interconnected. In the 10 min anodizing, a relatively uniform structure took shape. In the 30 min anodizing, however, an irregular dissolution of the pit walls on the alumina layer occurred, leading to an irregular structure. Surface morphology of the Al2024 after FPL-etching is presented in Fig. 6. As can be observed, the FPL-etching led to the formation of just about the same surface structure as in the 30 min anodized sample.

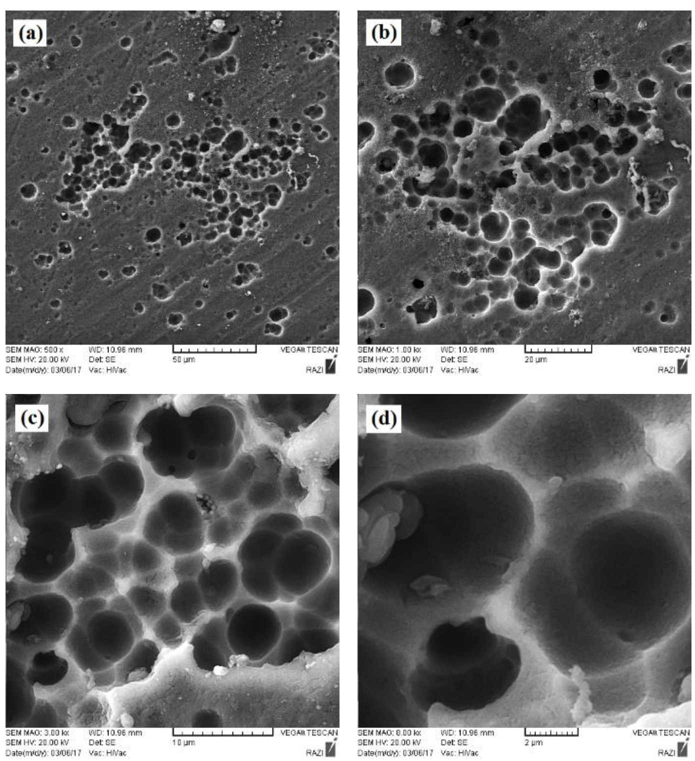

Fig. 6. The surface morphology of Al2024 after FPL-etching at different magnifications.

This is the accepted manuscript (postprint) of the following article:
Aghamohammadi, H., Abbandanak, S. N. H., Eslami-Farsani, R., & Siadati, S. H. (2018). Effects of various aluminum surface treatments on the basalt fiber metal laminates interlaminar adhesion. *International Journal of Adhesion and Adhesives*, *84*, 184-193.
https://doi.org/10.1016/j.ijadhadh.2018.03.005

3-2- Flexural testing

Flexural stress-strain curves of samples treated by various surface methods are illustrated in Fig. 8. It is evident that the flexural stress of the MA and Alkaline samples increased linearly until failure. Failure in the MA sample occurred at flexural strength and strain to failure of 396 MPa and 0.0055, respectively. This behavior is attributed to a weak interfacial bonding. In FMLs, typically, delamination occurs between the metal and the FRP layers. Therefore, adhesion at the metal/polymer interface plays a significant role in the mechanical properties of multicomponent laminates. In fact, the alkaline sample showed better flexural strength in comparison with the MA sample; its flexural strength and strain to failure were 489 MPa and 0.014, respectively. The better performance of the alkaline sample is attributed to the microscale flake like morphology generated on the Al2040 surface which caused better adhesion at the metal/polymer interface.

In comparison to the MA and alkaline samples, the FPL and anodized samples exhibited significant improvements in the strain to failure and toughness. In Fig. 7, the relatively similar flexural behaviors of the FPL and anodized samples are evident. Among all samples, the maximum flexural strength of about 623 MPa was achieved for the SAA10 sample. This value is about 55% higher than that for the MA sample (396 MPa). The flexural strengths of all samples are graphically shown in Fig. 8. The values of 586, 554, and 547 MPa were achieved for the FPL, SAA20, and SAA30 samples, respectively.

This is the accepted manuscript (postprint) of the following article:
Aghamohammadi, H., Abbandanak, S. N. H., Eslami-Farsani, R., & Siadati, S. H. (2018). Effects of various aluminum surface treatments on the basalt fiber metal laminates interlaminar adhesion. *International Journal of Adhesion and Adhesives*, *84*, 184-193.
https://doi.org/10.1016/j.ijadhadh.2018.03.005

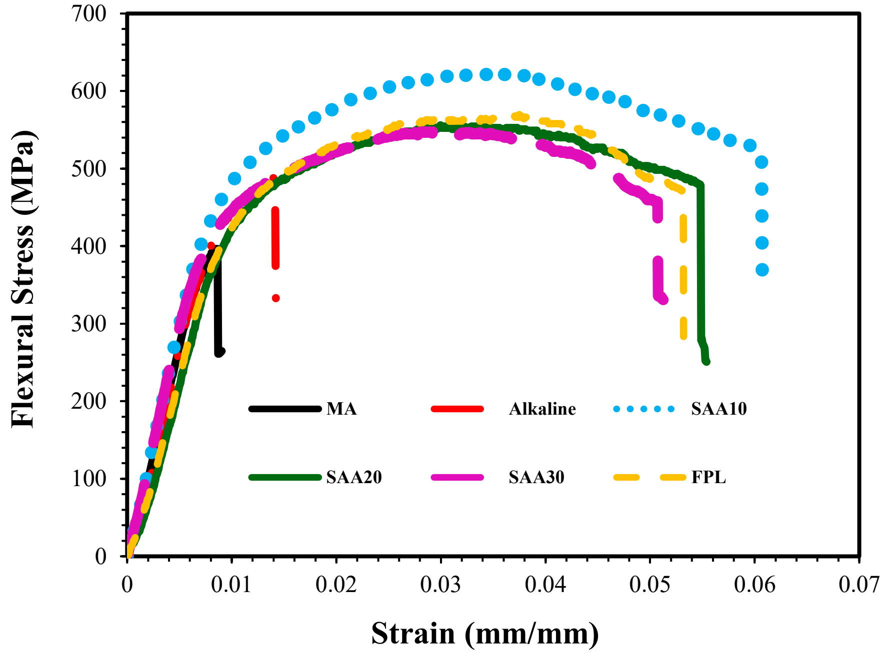

Fig. 7. Flexural stress-strain curves of basalt fibers/ epoxy/ aluminum 2024 laminates with different surface treatment methods.

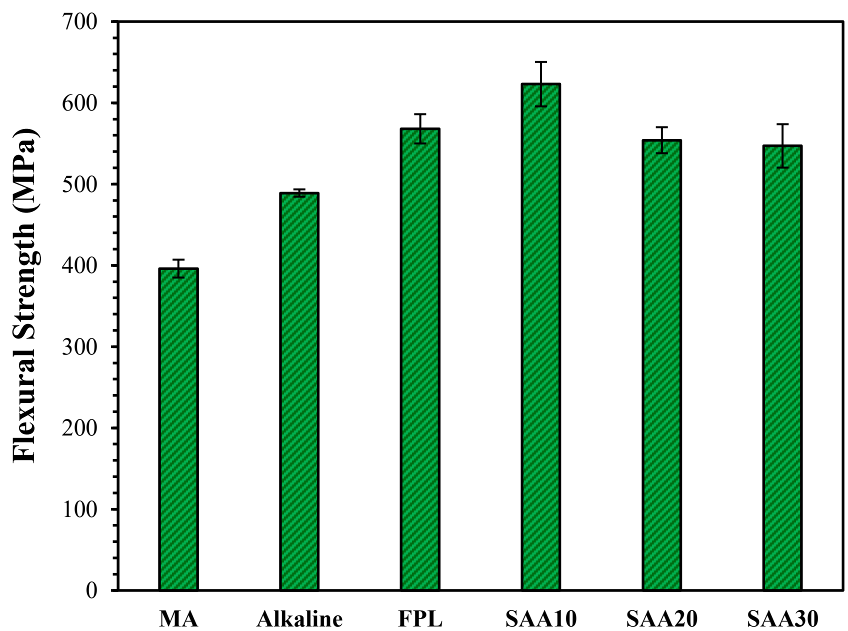

This is the accepted manuscript (postprint) of the following article:
Aghamohammadi, H., Abbandanak, S. N. H., Eslami-Farsani, R., & Siadati, S. H. (2018). Effects of various aluminum surface treatments on the basalt fiber metal laminates interlaminar adhesion. *International Journal of Adhesion and Adhesives*, *84*, 184-193.
https://doi.org/10.1016/j.ijadhadh.2018.03.005

Fig. 8. Flexural strength of basalt fibers/ epoxy/ aluminum 2024 laminates with different surface treatment methods.

The toughness values for all samples are graphically shown in Fig. 9. Comparing the surface area under the stress-strain curves for all samples, it is evident that the SAA10 sample has the highest value of about 32.3 J/mm^3 which is about 16 times larger than that for the MA sample (2.02 J/mm^3). This improvement is attributed to the presence of microscale pits formed on the surfaces of the FPL and anodized samples. The microscale pits provide proper and relatively uniform sites for resin penetration/infiltration during fabrication of the composites. This phenomenon causes the development of strong mechanical interlocking at the metal/polymer interface, hindering the easy occurrence of interfacial delamination during three-point bend test. The interface between aluminum and epoxy layers of the SAA10 sample is illustrated in Fig. 10 Clearly, there is a good adhesion between the layers.

This is the accepted manuscript (postprint) of the following article:
Aghamohammadi, H., Abbandanak, S. N. H., Eslami-Farsani, R., & Siadati, S. H. (2018). Effects of various aluminum surface treatments on the basalt fiber metal laminates interlaminar adhesion. *International Journal of Adhesion and Adhesives*, *84*, 184-193.
https://doi.org/10.1016/j.ijadhadh.2018.03.005

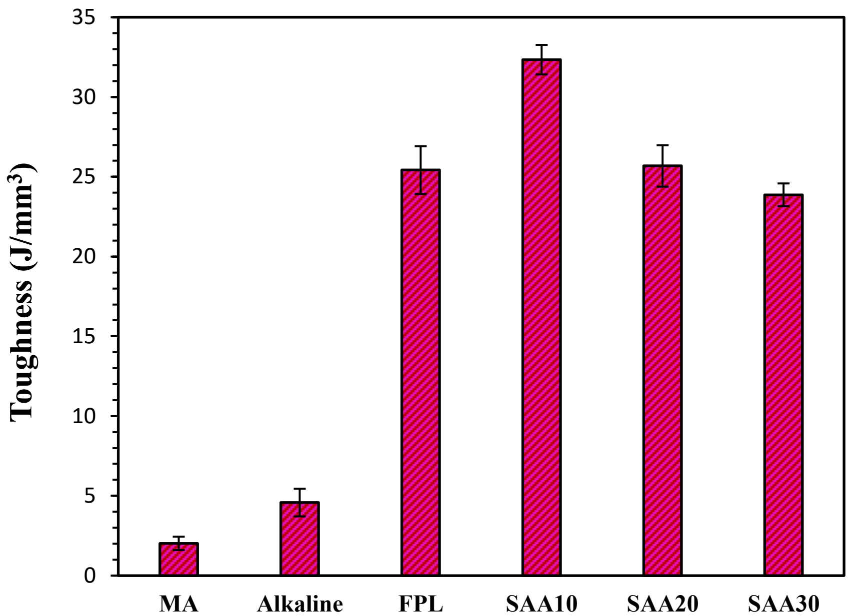

Fig. 9. Toughness of basalt fibers/ epoxy/ aluminum 2024 laminates with different surface treatment methods.

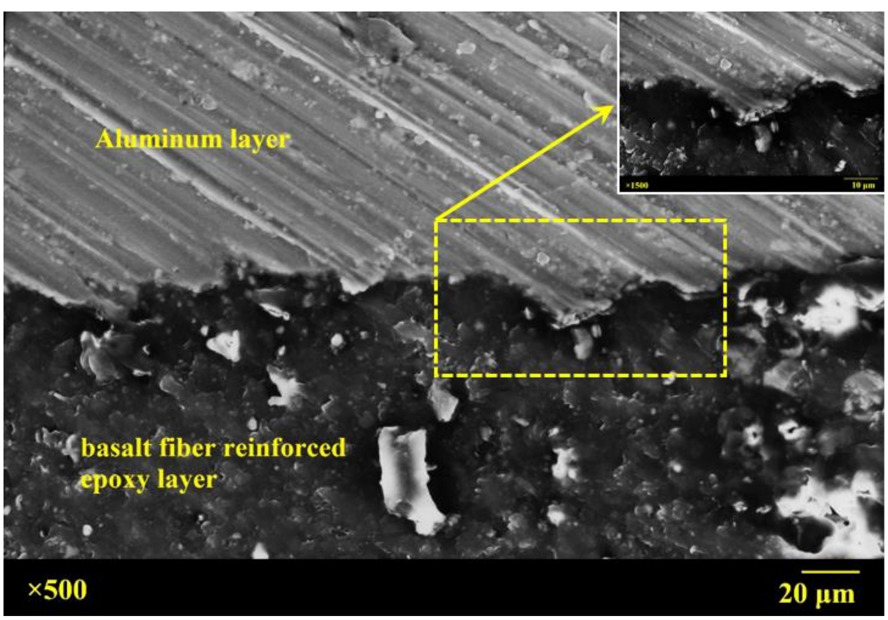

Fig. 10. SEM of the interface between aluminum 2024 and epoxy layers of sample treated for 10 min by SAA.

This is the accepted manuscript (postprint) of the following article:
Aghamohammadi, H., Abbandanak, S. N. H., Eslami-Farsani, R., & Siadati, S. H. (2018). Effects of various aluminum surface treatments on the basalt fiber metal laminates interlaminar adhesion. *International Journal of Adhesion and Adhesives*, *84*, 184-193.
https://doi.org/10.1016/j.ijadhadh.2018.03.005

In addition, it is well-known that the adhesive and cohesive failures are the main failure types of FMLs. Adhesive failure is related to the failure of the metal/polymer interface. On other hands, failure within the adhesive layer is introduced as the cohesive failure which is considered as the most desirable type of failure. The schematic illustration of these mechanisms are given in Fig. 11. The OM images of cross-section of different samples after bending tests are shown in Fig. 12. In Figs. 12 (a) and (b) the adhesive failure is observed for MA and Alkaline samples. In these samples the polymer/aluminum bond failed due to the occurrence of interfacial cracks. On other hands, the cohesive failure is the main failure type of SAA and FPL-etching samples. In other words, it can be said that there is a strong adhesion between aluminum and BFRP layers for SAA and FPL-etching samples.

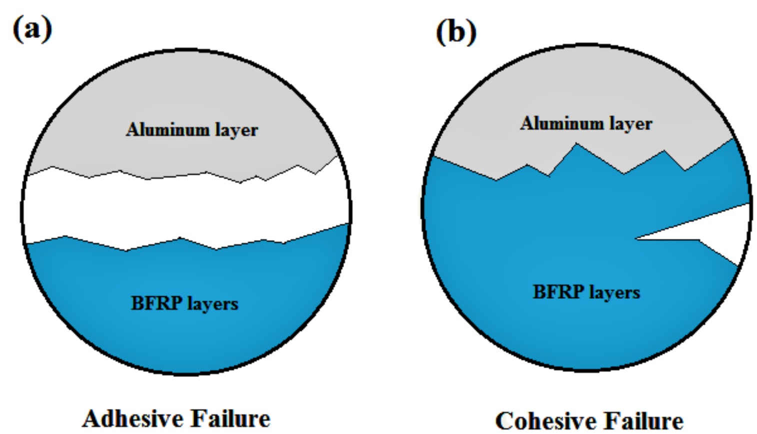

Fig. 11. Schematic illustration of the failure mechanisms of basalt fibers/ epoxy/ aluminum 2024 laminates.

This is the accepted manuscript (postprint) of the following article:
Aghamohammadi, H., Abbandanak, S. N. H., Eslami-Farsani, R., & Siadati, S. H. (2018). Effects of various aluminum surface treatments on the basalt fiber metal laminates interlaminar adhesion. *International Journal of Adhesion and Adhesives*, *84*, 184-193.
https://doi.org/10.1016/j.ijadhadh.2018.03.005

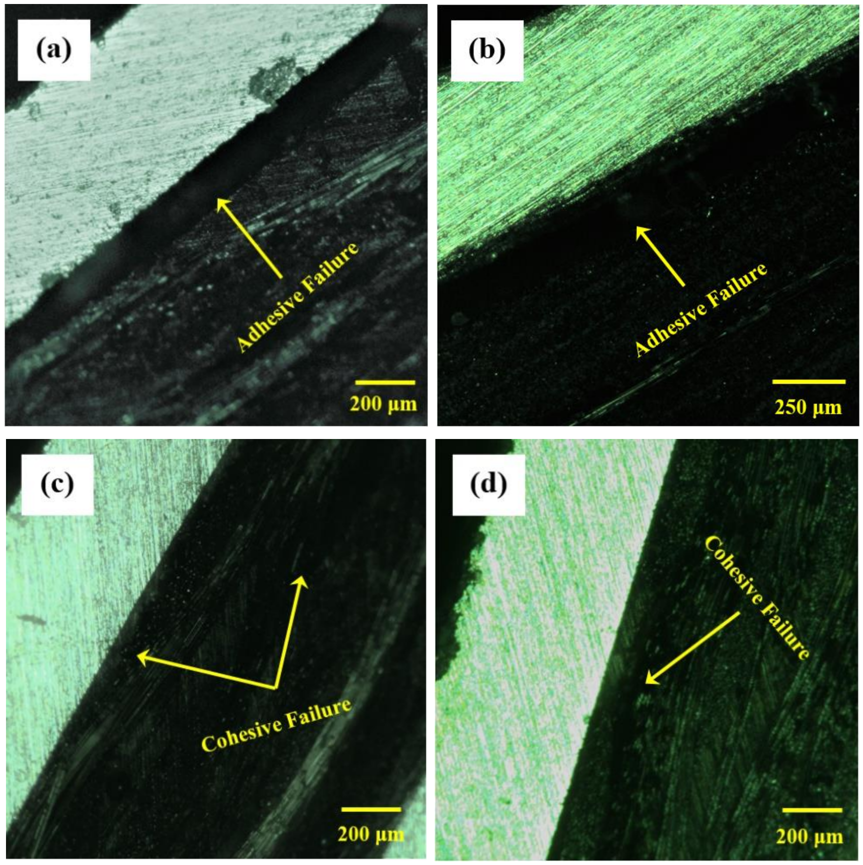

Fig. 12. SEM of the interface between aluminum 2024 and epoxy layers of (a) MA, (b) Alkaline, (c) SAA10 and (d) FPL-etching samples after bending test.

To better understand the failure mechanism of SAA and FPL-etching samples, the SEM images of aluminum fracture surfaces are depicted in Fig. 13. It can be seen that for SAA10 samples, there are the large number of BFRPs debris at the aluminum surface, demonstrating the occurrences of cohesive failure. However, for FPL-etching samples the remained BFRPs are much lower than those for SAA samples. In fact, it can be said that the failure types of SAA and FPL-etching samples are the combination of adhesive and cohesive. According to Fig. 13, the SAA10 samples failed more cohesively than FPL-etching samples.

This is the accepted manuscript (postprint) of the following article:
Aghamohammadi, H., Abbandanak, S. N. H., Eslami-Farsani, R., & Siadati, S. H. (2018). Effects of various aluminum surface treatments on the basalt fiber metal laminates interlaminar adhesion. *International Journal of Adhesion and Adhesives*, *84*, 184-193.
https://doi.org/10.1016/j.ijadhadh.2018.03.005

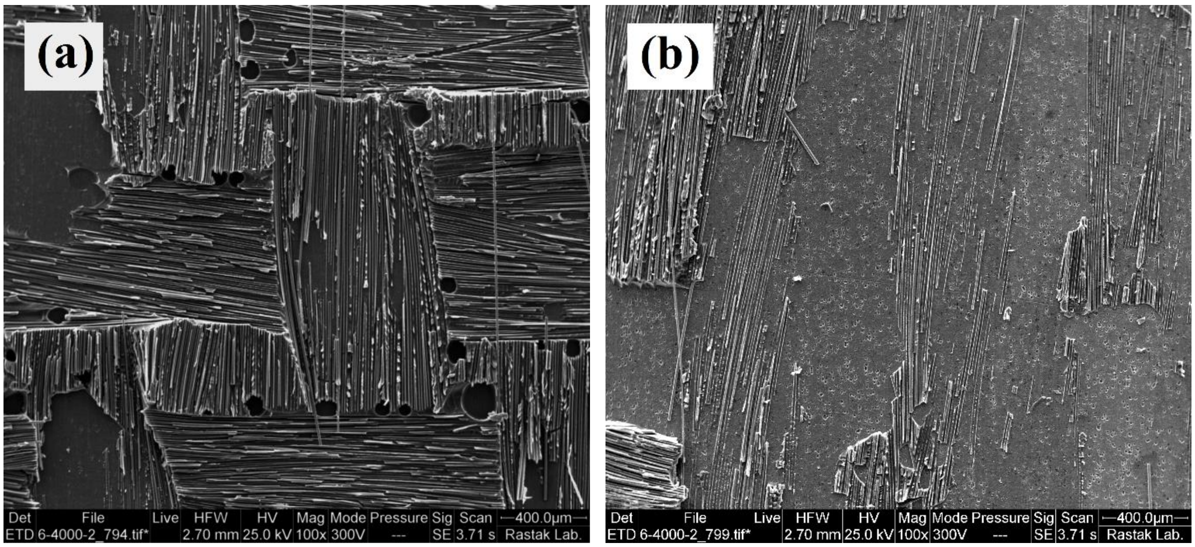

Fig. 13. The aluminum alloy fracture surface morphology of (a) SAA10 and (b) FPL-etching samples after bending test.

FMLs used in aircraft are subjects to the thermal cycling. Moreover, it is well-known that the coefficients of thermal expansions (CTE) of the aluminum and polymers are different. Therefore, it can be deduced that if the interface at metal/polymer was weak, these thermal cycles lead to the debonding of the FMLs. In summary, it can be said that the reliability of FMLs is strongly related to the metal/polymer interface. In this study, in addition to the strength values, the toughness values clearly indicate that the mechanical abrasion and alkaline methods are unsuitable for bonded joint applications.

Moreover, it is important to note that the time intervals used in this study indicated that beyond the 10 min anodizing, the flexural strength and toughness values decreased. As mentioned earlier, by increasing the anodizing time, the average pits' diameter increased, while the average pits spacing decreased. Shahzad et al. [19] compared the fatigue behavior of Al 7075 alloy with different surface treatments of pickling and CAA. After these treatments, surface morphology of aluminum composed of microscale pits due to the dissolution of second phases in Al 7075. They reported that the anodizing and pickling treatments respectively led to the 43% and 31% reduction

This is the accepted manuscript (postprint) of the following article:
Aghamohammadi, H., Abbandanak, S. N. H., Eslami-Farsani, R., & Siadati, S. H. (2018). Effects of various aluminum surface treatments on the basalt fiber metal laminates interlaminar adhesion. *International Journal of Adhesion and Adhesives*, *84*, 184-193.
https://doi.org/10.1016/j.ijadhadh.2018.03.005

of fatigue strength, comparing to the untreated samples. Their observations demonstrated that the pits were the most initiation sites for fatigue crack propagation. Accordingly, it can be deduced that with anodizing time increasing, the pits' diameter increases and consequently, became more proper sites for crack imitations.

In addition, this reaffirmed the results achieved by Zhang et al. [20]. They studied the effects of anodizing time on shear strengths of Al6061. They showed that beyond anodizing time of 20 min, the shear strength decreased. According to surface electron microscopy results, they concluded that excessive surface corrosion of Al6061 during anodizing beyond 20 min was the main reason for the drop in the shear strength. Therefore, there should be an optimum time span for the best adhesive strength in any particular system. This should be true for other parameters, too.

Another result is related to the flexural strength of the FPL sample. According to Figs. 5 and 6, it is evident that the average pit diameter in the FPL sample is larger than that of the SAA30 sample, and therefore it is expected that it's flexural strength to be inferior. However, as can be observed in Fig. 7, the FPL sample has better performance than both SAA20 and SAA30. Rougher surfaces of pit walls in the FPL sample could be the reason for this phenomenon. In fact, Mohamad et al. [15] has also reported that anodizing promoted a rougher surface and therefore better effect on the interfacial bonding.

A comparison between the surface roughness of the FPL and SAA10 samples is presented in Fig. 14. It is obvious that the pit walls of the FPL sample are rougher. Consequently, it was expected that the FPL sample would show better flexural strength, but the opposite turned out to be true. In this particular case, perhaps the lower flexural strength of the FPL sample could be attributed to the intense surface corrosion of the aluminum sheets.

This is the accepted manuscript (postprint) of the following article:
Aghamohammadi, H., Abbandanak, S. N. H., Eslami-Farsani, R., & Siadati, S. H. (2018). Effects of various aluminum surface treatments on the basalt fiber metal laminates interlaminar adhesion. *International Journal of Adhesion and Adhesives*, *84*, 184-193.
https://doi.org/10.1016/j.ijadhadh.2018.03.005

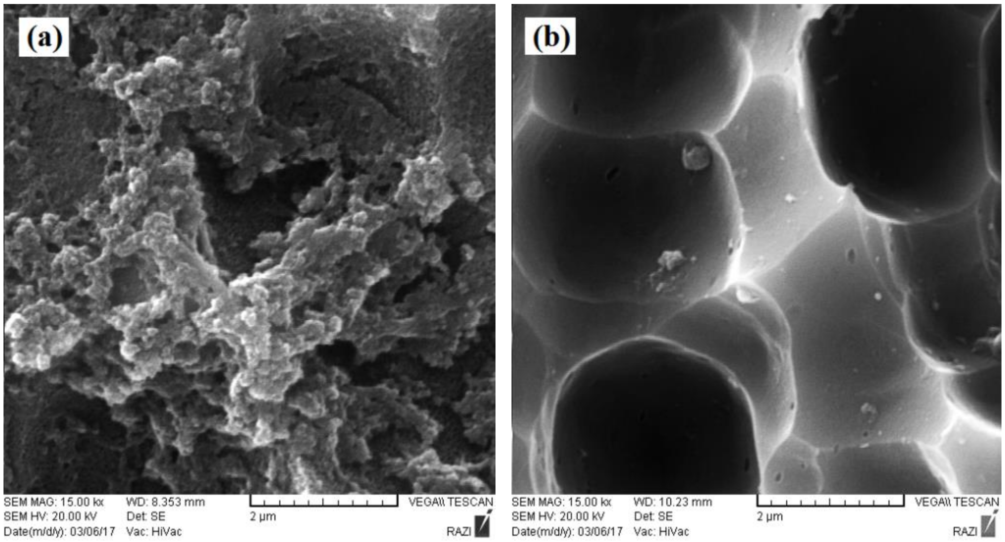

Fig. 14. Pit walls morphology of aluminum 2024 (a) FPL-etched, and (b) SAA10.

3-3- Profilometry testing

Surface roughness values of Al2024 after different times of SAA treatment are presented in Fig. 15. It shows a bell-shaped curve and the maximum occurred at 25 min. Surface roughness increased up to 25 min due to the presence of uniform pits on the oxide layer. The impact of anodizing time was earlier explained from the SEM images. In time, the average pit diameter increased in size, so did the surface roughness. But beyond 25 min, the pits became interconnected due to an irregular dissolution of the pit walls on the alumina layer, leading to an irregular structure and thus a downward trend in the surface roughness. These results coincide with those achieved by Mohamad et al. [15].

This is the accepted manuscript (postprint) of the following article:
Aghamohammadi, H., Abbandanak, S. N. H., Eslami-Farsani, R., & Siadati, S. H. (2018). Effects of various aluminum surface treatments on the basalt fiber metal laminates interlaminar adhesion. *International Journal of Adhesion and Adhesives*, *84*, 184-193.
https://doi.org/10.1016/j.ijadhadh.2018.03.005

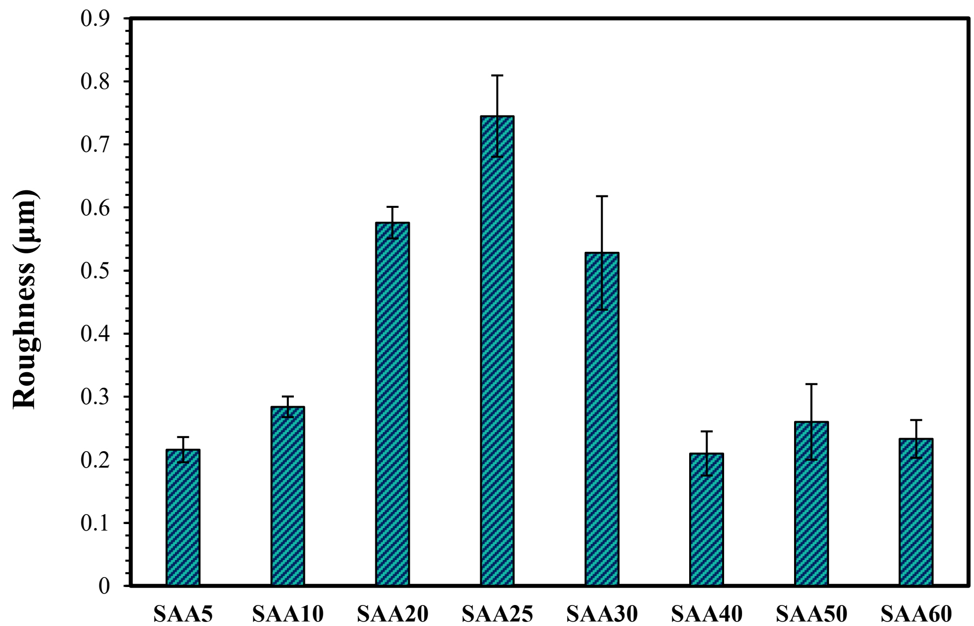

Fig. 15. Surface roughness of aluminum 2024 layer after SAA treatment at various times.

Based on the fact that higher roughness promotes higher surface area for bonding, it was expected that the SAA25 sample would have the highest flexural strength. However, the highest flexural strength was achieved for the SAA10 sample although its surface roughness was 77% smaller. Therefore, it can be concluded that among the various parameters affecting the adhesive strength of dissimilar parts, the optimum conditions differ for each case in order to achieve the best mechanical behavior.

4- Conclusions

In this research, the effects of four different surface treatment methods of mechanical abrasion, alkaline etching, FPL-etching and sulfuric acid anodizing on the mechanical properties of basalt fibers/epoxy/aluminum 2024 laminates were studied. Surface roughness and mechanical testing such as profilometry and flexural testing were performed and the following conclusions were drawn:

1- The flexural behaviors of the samples treated with mechanical abrasion and alkaline etching were totally elastic and that delamination between Al2024 and basalt fiber reinforced polymer layers occurred at the maximum flexural stress. These results indicated that the grinding and alkaline treatment methods create poor bonding between the layers and therefore are not suitable for adhesive bonding applications. Moreover, fracture analyses showed that the adhesive failure was occurred for mechanical abrasion and alkaline etching samples.

2- The FPL-etching and sulfuric acid anodizing treatments caused significant improvements in the strain to failure and toughness values, compared to the mechanical abrasion and alkaline etching treatments. The presence of microscale pits caused by etching treatment on the Al2024 surface was the main cause of these improvements. The microscale pits provided sites for infiltration of the epoxy resin, creating strong mechanical interlocking between the alternating laminates. In addition, the fracture analyses indicated that the combination of the adhesive and cohesive failure was occurred for FPL-etching and anodized samples.

3- Anodizing time played a great role on the morphology of the anodized samples; the dissolution rate increased in time leading to increase in the pit size and roughness of the aluminum oxide layer. Although higher surface roughness provides larger surface area useful for adhesive bonding, there is a limit beyond which degradation occurs, i.e., there must be an optimal anodizing time. In this study, the sample treated with sulfuric acid anodizing for 10 min exhibited better flexural properties than those treated for 20 and 30 min, although the latter possessed higher surface roughness.

References

[1] G.B. Chai, P. Manikandan, Low velocity impact response of fibre-metal laminates–A review, Composite Structures 107 (2014) 363-381.

[2] T. Sinmazçelik, E. Avcu, M.Ö. Bora, O. Çoban, A review: Fibre metal laminates, background, bonding types and applied test methods, Materials & Design 32(7) (2011) 3671-3685.

This is the accepted manuscript (postprint) of the following article:
Aghamohammadi, H., Abbandanak, S. N. H., Eslami-Farsani, R., & Siadati, S. H. (2018). Effects of various aluminum surface treatments on the basalt fiber metal laminates interlaminar adhesion. *International Journal of Adhesion and Adhesives*, *84*, 184-193.
https://doi.org/10.1016/j.ijadhadh.2018.03.005

[3] R.E. Farsani, S.M.R. Khalili, V. Daghigh, Charpy impact response of basalt fiber reinforced epoxy and basalt fiber metal laminate composites: Experimental study, International Journal of Damage Mechanics 23(6) (2013) 729-744.

[4] L. Ferrante, F. Sarasini, J. Tirillò, L. Lampani, T. Valente, P. Gaudenzi, Low velocity impact response of basalt-aluminium fibre metal laminates, Materials & Design 98 (2016) 98-107.

[5] S. Khalili, V. Daghigh, R. Eslami Farsani, Mechanical behavior of basalt fiber-reinforced and basalt fiber metal laminate composites under tensile and bending loads, Journal of Reinforced Plastics and Composites 30(8) (2011) 647-659.

[6] E. Botelho, R. Silva, L. Pardini, M. Rezende, Evaluation of adhesion of continuous fiber–epoxy composite/aluminum laminates, Journal of adhesion science and technology 18(15-16) (2004) 1799-1813.

[7] M. Ostapiuk, B. Surowska, J. Bieniaś, Interface analysis of fiber metal laminates, Composite Interfaces 21(4) (2013) 309-318.

[8] Y. Xu, H. Li, Y. Shen, S. Liu, W. Wang, J. Tao, Improvement of adhesion performance between aluminum alloy sheet and epoxy based on anodizing technique, International Journal of Adhesion and Adhesives 70 (2016) 74-80.

[9] S.Y. Park, W.J. Choi, H.S. Choi, H. Kwon, S.H. Kim, Recent Trends in Surface Treatment Technologies for Airframe Adhesive Bonding Processing: A Review (1995–2008), The Journal of Adhesion 86(2) (2010) 192-221.

[10] M. Mohamad, H.F.A. Marzuki, E. Ubaidillah, M. Abidin, S. Omar, I. Rozi, Effect of Surface Roughness on Mechanical Properties of Aluminium-Carbon Laminates Composites, Advanced Materials Research, Trans Tech Publ, 2014, pp. 51-57.

[11] D. Arrowsmith, A. Clifford, Morphology of anodic oxide for adhesive bonding of aluminum, International journal of adhesion and adhesives 3(4) (1983) 193-196.

[12] J. Venables, D. McNamara, J. Chen, T. Sun, R. Hopping, Oxide morphologies on aluminum prepared for adhesive bonding, Applications of Surface Science 3(1) (1979) 88-98.

[13] G. Lawcock, L. Ye, Y.-W. Mai, C.-T. Sun, The effect of adhesive bonding between aluminum and composite prepreg on the mechanical properties of carbon-fiber-reinforced metal laminates, Composites Science and Technology 57(1) (1997) 35-45.

[14] S.G. Prolongo, A. Ureña, Effect of surface pre-treatment on the adhesive strength of epoxy–aluminium joints, International Journal of Adhesion and Adhesives 29(1) (2009) 23-31.

[15] M. Mohamad, H.F.A. Marzuki, S.N.A. Bakar, A.N. Abdullah, E.A.E. Ubaidillah, M.F.Z. Abidin, S. Omar, Effect of Anodizing Electrolyte for Structural Adhesives Bonding Study of Aluminium-Carbon Laminates Composites, International Journal of Automotive and Mechanical Engineering 10 (2014) 2091-2101.

[16] A. Datta, R.A. Pethrick, S. Affrossman, Surface Analysis of Etched and Anodised Aluminium-Copper Alloys, The Journal of Adhesion 15(1) (2007) 13-25.

[17] N. Fin, H. Dodiuk, A. Yaniv, L. Drori, Oxide treatments of Al 2024 for adhesive bonding-surface characterization, Applied surface science 28(1) (1987) 11-33.

[18] M.S. de Miera, M. Curioni, P. Skeldon, G. Thompson, The behaviour of second phase particles during anodizing of aluminium alloys, Corrosion Science 52(7) (2010) 2489-2497.

[19] M. Shahzad, M. Chaussumier, R. Chieragatti, C. Mabru, F. Rezai-Aria, Surface characterization and influence of anodizing process on fatigue life of Al 7050 alloy, Materials & Design 32(6) (2011) 3328-3335.

[20] Z. Zhang, J.-G. Shan, X.-H. Tan, J. Zhang, Effect of anodizing pretreatment on laser joining CFRP to aluminum alloy A6061, International Journal of Adhesion and Adhesives 70 (2016) 142-151.